J. Solid Mech. 2026; 18(01): 1-14

Journal of Solid Mechanics

https://doi.org/10.57647/jsm.2026.1801.01

Research Article

Stress Analysis for FGM Sphere in the Couple Stress Elasticity

Foad Saadi, Mohsen Jabbari*, Mehdi Yarmohammad Tooski

Department of Mechanical Engineering, ST.C., Islamic Azad University, Tehran, Iran

***Corresponding author:** m_jabbari@azad.ac.ir

Article History:

Received:
18 December 2025

Revised:
26 February 2026

Accepted:
20 March 2026

Published in Issue:
31 March 2026

Abstract

This study develops an analytical framework based on Modified Couple Stress Theory (MCST) to investigate the stress response of functionally graded hollow spheres. The governing equations, which consider both material gradation and microstructural length-scale parameters, are solved with high accuracy using the Generalized Differential Quadrature (GDQ) method. The proposed framework exhibits numerical stability and strong convergence, and shows excellent agreement with benchmark analytical solutions reported in the literature, with a deviation of less than 3%. For a microstructural length-scale parameter of 0.1 µm, the results are in close agreement with classical elasticity predictions, with a deviation of less than 2%, confirming the robustness and reliability of the formulation in a multiscale context. Furthermore, increasing the material gradient index increases the sensitivity of the stress to the length-scale parameter, highlighting the coupling between material composition and microstructural effects. This integrated MCST-GDQ approach provides a solid and efficient foundation for further research on microstructured materials, smart composites, and multiscale mechanical systems.

Keywords: Functionally graded materials (FGM); Couple stress theory; Modified Couple Stress Theory (MCST); Hollow sphere; Generalized Differential Quadrature (GDQ); Microstructural Length Scale

Cite this article: Saadi, F., Jabbari, M., Yarmohammad Tooski, M., (2026). Stress Analysis for FGM Sphere in the Couple Stress Elasticity, *Journal of Solid Mechanics,* 18(01): 1-14. https://doi.org/10.57647/jsm.2026.1801.01

1. Introduction

Functionally Graded Materials (FGMs) are a revolutionary development in the field of materials science because their composition or structure gradates from one point to another.

As a result, the physical and mechanical properties can only have a gradual variation. This has proven useful in making the materials more resistant to distinct environmental factors. The materials have distinct applications across many sectors. In the aerospace field, for instance, FGMs reduce the effect of mass on the structure. They thereby increase the structure's ability to withstand heat and pressure. In the health field, the materials aim at simulating the human tissue [1]. In addition, Stress analysis of FGMs is more complicated due to the variation in their mechanical properties.

The analysis of the behavior of the materials under different loading states through the use of numerical techniques like the GDQ method can assist in understanding how the materials react to environmental and internal loading [2].

2. Importance and necessity of research

Analysis of stress in Functional Graded Materials (FGMs), especially when the couple stress elasticity concept comes into play, has a great significance and urgency because of the complexity involved in the stress and strain behavior of the materials. An accurate analysis of the stress behavior of the materials can translate to improved safety and performances of the structures designed.

The demand to comprehend and analyze the intricacies involved in the elastic behavior of materials like FGMs, especially when subjected to varying loading patterns and factors, has made the adoption of latest techniques and tools related to stress analysis more important than ever before.

Accurate analyses of stress can assist the designer in improving their designs based on the weaknesses present in the structure [3].

On the other hand, the stress analysis of FGMs under couple stress elasticity can become challenging because of the complexities involved due to the specific nature of the materials' characteristics and the requirements for high accuracy in the results of their elastic behavior. In order to overcome the above-mentioned challenges and complexities, more research and development in innovative tools and methodologies will be required.

3. Research objectives

The main objectives of this research include the following:

- Development of an analytical–numerical model for stress analysis of functionally graded spherical structures based on MCST
- Examination of the elastic behavior of FGM spheres under various loading conditions
- Analysis of the influence of material gradation and length-scale parameters using the GDQ method

4. Methodology

In the context of stress analysis for functionally graded materials (FGMs), the importance of analytical and numerical solutions cannot be overemphasized for a deeper understanding of the materials' behavior and benefiting from the optimized properties of the materials, particularly in the context of certain couple stress elasticity problems.

Since the material properties are varied, the analysis of FGMs must be carried out in an accurate manner to forecast the behavior of the materials under varied conditions of loading. Conventionally, analytical solutions are used to handle the difficulties associated with the analysis of FGM materials. In the process, the partial differential equations (PDEs), which explain the elastic behavior of the materials, are solved.

While the solutions obtained may result in high accuracies, most of the methods are valid for limited conditions only.

For example, in the process of stress analysis for spherical problems, Legendre functions are applicable; these functions are very useful for solving the equations for FGMs during static and dynamic loading conditions. With regard to the analysis process, the analytical approach remains less efficient compared to the numerical approach, particularly in a complex condition. Among the popular techniques used for the analysis of stresses in FGM using the numerical approach is the Generalized Differential Quadrature technique.

The GDQ approach facilitates the high accuracy calculation of the stress and strain distribution in FGMs without the complexity associated with the geometrical discretization of the body's geometric representation. Its capability to utilize the difference and integral forms of the basis functions makes the GDQ approach capable of solving the nonlinear equations associated with the stresses within the body for various loads.

Other advantages of the GDQ approach lie in the fact that it can be combined with other numerical techniques, such as the Finite Element Method (FEM).

The application of analytical and numeric techniques in studying the behavior of functionally graded materials (FGMs) based on couple stress elasticity not only aids in the investigation of such materials, but it also contributes towards an enhanced comprehension of the distinct properties associated with these materials [4].

5. Review of the research literature

The elasticity of couple stress in FGMs can be considered within the framework of two broad areas: analytical and numerical analyses.

Various studies in the early years targeted the analysis of stress and strain in FGMs using analytical methods.

For example, in their 1998 book, Suresh and Mortensen [5] discussed mechanical behavior and properties of FGMs and proposed different analytical models under specific conditions.

Under such models, the development was done under simple loading conditions and for certain examples; however, due to limitations in the complexity of real conditions, they achieved limited effectiveness.

Noori and Jomehzadeh [6] considered the length-scale effect on vibration of functionally graded Kirchhoff and Mindlin micro-plates and showed how the intrinsic length parameters influence the natural frequencies in FGM microplates.

As the numerical technologies advanced, the researchers started focusing on numerical methods to study the behavior of FGMs.

The finite element method (FEM) is considered one of the most popular methods, and therefore, many studies have involved the use of this method, with one important study by Yas et al., published in 2011, addressing stress and displacement analysis in various configurations [7].

A few analytical and semi-analytical solutions of scaledependent structures have also appeared in IJE. An example is a recent analytical solution of free vibration of nonuniform microbeams which implemented modified couple-stress theory to capture size effects on frequencies [8].

Tornabene and Viola [9] employed the generalized differential quadrature method to obtain highly accurate solutions for the vibration behavior of shell structures with curved geometries.

Their formulation, based on classical elasticity, established GDQ as a powerful alternative to conventional numerical methods for spherical and parabolic shells.

Nevertheless, their study did not incorporate modified couple stress theory or any form of size-dependent elasticity, and therefore cannot predict micro-scale stiffening effects observed in small-scale spherical structures.

Very recently, Wu and Chang [10] reviewed several formulations of couple stress and strain gradient for FG microstructures. The MCST is verified to balance accuracy and computational efficiency.

Tadi Beni et al. worked on size effects in piezoelectric nano-beam type FGM energy harvesters and reported pronounced length-scale dependence in both static and dynamic responses [11]. Besides, Forghani et al. [12] investigated the nonlinear resonances of FG-GPLRC cylindrical shells subjected to thermal environments, which demonstrated that symmetric grading patterns minimize amplitude peaks, a concept well transferrable to spherical geometries. From this perspective, Rashvand et al.'s study [13] have indicated that, within the electro-mechanical framework, the intrinsic length-scale parameter significantly influences pull-in voltage and the mechanical stability of electrostatically actuated FGM microplates. Within the last few years, advanced methods like the Generalized Differential Quadrature (GDQ) method and techniques such as the Boundary Element Method (BEM) have been adopted for the analysis of FGMs. Relevant investigations also combined the couple-stress formulations with electro-mechanical and adsorption problems, e.g., couple stress modeling of micro/nano-cantilever capacitive sensors to capture size-dependent behavior under surface effects [14].

Since FGMs have unique properties and a wide range of applications, the stress analysis of functionally graded materials has become one of the important focuses of research in engineering.

Some researchers have attempted to develop mathematical models that can properly represent the mechanical behavior of FGMs with due consideration for microstructural effects.

Farokhi and Ghayesh [15], in a study, modified the strain gradient and couple-stress theories in curvilinear coordinates.

The authors developed mathematical models and performed numerical simulations to investigate the accuracy of the stress-strain predictions and discussed the influence of current parameters on mechanical properties and compared experimental results with the proposed models.

Bleustein [16] discussed the effects of microstructure on stress concentration arising around spherical cavities.

The numerical models employed by him to simulate the distribution of stress in samples with different microstructures, using FEM, indicate that features as grain size and distribution play a crucial role in stress concentration and thus determine the failure potential. Zhao et al. [17], in the development of the theory for strain gradients in curved coordinates, introduced the equilibrium equations and boundary conditions, pointing out the importance of microstructural effects and providing suitable conditions for simulation models. The modified couple stress theory was used for the analysis of vibrations in microplates by Jomehzadeh et al. [18].

Their new mathematical model took into consideration size and microstructure effects on dynamic properties, enabling a more detailed analysis of the vibrational behavior and numerical simulations to verify the model.

Nateghi et al. [19] discussed the stability of functionally graded microbeams with size-dependent behavior.

They developed a model incorporating microstructural and material composition variations for the accurate prediction of buckling response.

Reddy [20] discussed the couple stress theories associated with microstructure for functionally graded beams, while analyzing natural frequencies, buckling loads, and dynamic responses, considering the influence of microstructural effects.

Reddy and Kim [21] developed a modified couple-stress-based third-order nonlinear theory for FG plates considering size dependence and nonlinearity of mechanical behavior; through numerical analyses, their works showed that these theories provide improved

accuracy in the prediction of buckling and vibrational responses.
Sadeghi et al. [22] analyzed the stress-strain in functional microbeams by using gradient elasticity theory, pointing out the influences of scale variation and material properties. Salamat-talab et al. [23] considered the surface energy and gradient elasticity in the study of size-dependent behavior of functional beams and demonstrated evident effects on buckling and vibrational responses at small-scales.

6. Research innovation

This study presents an integrated analytical-numerical approach to investigate the stress distribution in functionalized materials (FGM), where the material composition changes inside the structure.
This approach integrates classical formulations with advanced numerical methods, namely the GDQ method. It aims to provide a deep understanding of the mechanical response of functional materials, validate numerical results with respect to mechanical loading, fill the gaps in existing research in this field, and enhance the predictive capability for strength evaluation.
Therefore, the present work investigates for the first time the problem of non-uniform internal stress applied to a micro-scale spherical structure composed of material properties with spatial variations.
The applied stress varies by 400 times the cosine of the polar angle acting on the inner surface of the sphere. Such a form of non-uniform loading naturally generates ambiently varying stress fields and allows for a deep analysis of local stress concentrations and anisotropic effects, which are usually neglected in most analyses.
The scale-sensitive analysis method presented here, by considering size-dependent effects in the framework of coupled-stress elasticity using the GDQ technique, provides a more accurate representation of the mechanical response in microscale structures.
This method allows for the analysis of scale sensitivity, geometric variations, and nonuniform loading effects simultaneously.
This work addresses one of the important challenges in micro- and Nano engineering: how to predict stress concentration and potential failure in very small components.
The developed model increases the reliability of stress analysis in MEMS, miniature pressure vessels, and spacecraft thermal protection systems, where both nonuniform pressure effects and size effects significantly affect the performance of the structure.

7. Three-dimensional governing equations of the modified couple-stress theory in spherical coordinates

At micro and smaller scales, the results obtained from theory and experiments in stress and strain analyses differ from each other. The main reason for this issue is the inadequacy of classical elasticity theory, which is unable to describe the size effect on material properties at small scales. In other words, classical continuum mechanics cannot account for the Length Scale Parameter in governing relations. To address this deficiency, many generalized continuum theories have been proposed.
Among these theories, modified couple-stress theories and modified strain gradient theories have achieved significant success. In the study conducted by Ashoori and Mahmoodi [24], the modified strain gradient theory has been derived in detail in general curved coordinates.
The modified strain gradient theory encompasses the modified couple-stress theory as a special case. Accordingly, the modified couple-stress theory is derived in general curved coordinates, and the results are then specialized for practical orthogonal curved coordinates, namely spherical coordinates. Expressions including deformation criteria, governing equations, boundary conditions, and constitutive equations are presented in terms of physical components that are more common and convenient. The use of curved coordinates in tensile plate problems involving cylindrical and spherical cavities, crack analysis, interpretation of Micro/Nano indentation tests, as well as bending or torsion tests at small scales is inevitable. The three-dimensional equations governing the coupled stress theory in spherical coordinates are defined as follows [24]:

$$\frac{\partial \psi_{rr}}{\partial r}+\frac{1}{r}\frac{\partial \psi_{\theta r}}{\partial \theta}+\frac{1}{r\,sin\,\theta}\frac{\partial \psi_{\varphi r}}{\partial \varphi}+ \frac{1}{r}\left(2\psi_{rr}-\psi_{\theta\theta}-\psi_{\varphi\varphi}+\psi_{\theta r}\,cot\,\theta\right)+f_r=0 \quad (1)$$

$$\frac{\partial \psi_{r\theta}}{\partial r}+\frac{1}{r}\frac{\partial \psi_{\theta\theta}}{\partial \theta}+\frac{1}{r\,sin\,\theta}\frac{\partial \psi_{\varphi\theta}}{\partial \varphi}+ \frac{1}{r}\left(2\psi_{r\theta}+\psi_{\theta r}+(\psi_{\theta\theta}-\psi_{\varphi\varphi})\,cot\,\theta\right)+f_\theta=0 \quad (2)$$

$$\frac{\partial \psi_{r\varphi}}{\partial r}+\frac{1}{r}\frac{\partial \psi_{\theta\varphi}}{\partial \theta}+\frac{1}{r\,sin\,\theta}\frac{\partial \psi_{\varphi\varphi}}{\partial \varphi}+ \frac{1}{r}\left(2\psi_{r\varphi}+\psi_{\varphi r}+\psi_{\varphi\theta}\,cot\,\theta\right)+f_\varphi=0 \quad (3)$$

10.57647/jsm.2026.1801.01

In the above relationships, $f_i(i = r, \theta, \varphi)$ the stresses are volumetric and $\psi_{ij}(i, j = r, \theta, \varphi)$ are defined as follows:

$$\psi_{rr} = \sigma_{rr} - \left(\begin{array}{l} \frac{\partial p_r}{\partial r} + \frac{\partial \tau^{[1]}_{rrr}}{\partial r} + \frac{1}{r}\frac{\partial \tau^{[1]}_{rr\theta}}{\partial \theta} + \frac{1}{r\sin\theta}\frac{\partial \tau^{[1]}_{rr\varphi}}{\partial \varphi} + \\ \frac{1}{r}\left(2\tau^{[1]}_{rrr} - 2\tau^{[1]}_{r\theta\theta} - 2\tau^{[1]}_{r\varphi\varphi} + \tau^{[1]}_{rr\theta}\cot\theta\right) \\ +\frac{1}{2}\left(\frac{1}{r\sin\theta}\frac{\partial m_{r\theta}}{\partial \varphi} - \frac{1}{r}\frac{\partial m_{r\varphi}}{\partial \theta} - \frac{m_{r\varphi}}{r}\cot\theta\right) \end{array}\right)$$

$$\psi_{r\theta} = \sigma_{r\theta} - \left(\begin{array}{l} \frac{1}{r}\frac{\partial p_r}{\partial \theta} - \frac{p_\theta}{r} + \frac{\partial \tau^{[1]}_{rr\theta}}{\partial r} + \\ \frac{1}{r}\frac{\partial \tau^{[1]}_{r\theta\theta}}{\partial \theta} + \frac{1}{r\sin\theta}\frac{\partial \tau^{[1]}_{r\theta\varphi}}{\partial \varphi} \\ +\frac{1}{r}\left(\begin{array}{l} 3\tau^{[1]}_{rr\theta} - \tau^{[1]}_{\theta\theta\theta} - \tau^{[1]}_{\theta\varphi\varphi} \\ +\tau^{[1]}_{r\theta\theta}\cot\theta - \tau^{[1]}_{r\varphi\varphi}\cot\theta \end{array}\right) + \\ \frac{1}{2}\left(\frac{\partial m_{r\varphi}}{\partial r} - \frac{1}{r\sin\theta}\frac{\partial m_{rr}}{\partial \varphi} + \frac{2m_{r\varphi}}{r}\right) \end{array}\right) \quad (4)$$

$$\psi_{r\varphi} = \sigma_{r\varphi} - \left(\begin{array}{l} \frac{1}{r\sin\theta}\frac{1}{r}\frac{\partial p_r}{\partial \varphi} - \frac{p_\varphi}{r} + \frac{\partial \tau^{[1]}_{rr\varphi}}{\partial \theta} \\ +\frac{1}{r}\frac{\partial \tau^{[1]}_{r\theta\varphi}}{\partial \theta} + \frac{1}{r\sin\theta}\frac{\partial \tau^{[1]}_{r\varphi\varphi}}{\partial \varphi} \\ +\frac{1}{r}\left(\begin{array}{l} 3\tau^{[1]}_{rr\varphi} - \tau^{[1]}_{\varphi\varphi\varphi} - \tau^{[1]}_{\theta\varphi\varphi} + \\ \tau^{[1]}_{\theta\theta\varphi} + 2\tau^{[1]}_{r\theta\varphi}\cot\theta \end{array}\right) + \\ \frac{1}{2}\left(\frac{1}{r}\frac{\partial m_{rr}}{\partial \theta} - \frac{\partial m_{r\theta}}{\partial r} - \frac{2m_{r\theta}}{r}\right) \end{array}\right)$$

$$\psi_{\theta r} = \sigma_{\theta r} - \left(\begin{array}{l} \frac{\partial p_\theta}{\partial r} + \frac{\partial \tau^{[1]}_{rr\theta}}{\partial r} + \frac{1}{r}\frac{\partial \tau^{[1]}_{r\theta\theta}}{\partial \theta} \\ +\frac{1}{r\sin\theta}\frac{\partial \tau^{[1]}_{r\theta\varphi}}{\partial \varphi} \\ +\frac{1}{r}\left(\begin{array}{l} 3\tau^{[1]}_{rr\theta} - \tau^{[1]}_{\theta\theta\theta} - 2\tau^{[1]}_{\theta\varphi\varphi} \\ +\tau^{[1]}_{r\theta\theta}\cot\theta - \tau^{[1]}_{r\varphi\varphi}\cot\theta \end{array}\right) \\ +\frac{1}{2}\left(\begin{array}{l} \frac{1}{r\sin\theta}\frac{\partial m_{\theta\theta}}{\partial \varphi} - \frac{1}{r}\frac{\partial m_{\theta\varphi}}{\partial \theta} \\ -\frac{m_{r\varphi}}{r} - \frac{2m_{\theta\varphi}}{r}\cot\theta \end{array}\right) \end{array}\right) \quad (5)$$

$$\psi_{\theta\theta} = \sigma_{\theta\theta} - \left(\begin{array}{l} \frac{1}{r}\frac{\partial p_\theta}{\partial \theta} + \frac{p_r}{r} + \frac{\partial \tau^{[1]}_{r\theta\theta}}{\partial r} + \\ \frac{1}{r}\frac{\partial \tau^{[1]}_{\theta\theta\theta}}{\partial \theta} + \frac{1}{r\sin\theta}\frac{\partial \tau^{[1]}_{\theta\theta\varphi}}{\partial \varphi} \\ +\frac{1}{r}\left(\begin{array}{l} 4\tau^{[1]}_{r\theta\theta} + \tau^{[1]}_{\theta\theta\theta}\cot\theta \\ -2\tau^{[1]}_{\theta\varphi\varphi}\cot\theta \end{array}\right) \\ +\frac{1}{2}\left(\begin{array}{l} \frac{\partial m_{\theta\varphi}}{\partial r} - \frac{1}{r\sin\theta}\frac{\partial m_{r\theta}}{\partial \varphi} \\ +\frac{m_{\theta\varphi}}{r} + \frac{2m_{r\varphi}}{r}\cot\theta \end{array}\right) \end{array}\right)$$

$$\psi_{\theta\varphi} = \sigma_{\theta\varphi} - \left(\begin{array}{l} \frac{1}{r\sin\theta}\frac{\partial p_\theta}{\partial \varphi} - \frac{p_\varphi}{r}\cot\theta + \frac{\partial \tau^{[1]}_{r\theta\varphi}}{\partial r} \\ +\frac{1}{r}\frac{\partial \tau^{[1]}_{\theta\theta\varphi}}{\partial \theta} + \frac{1}{r\sin\theta}\frac{\partial \tau^{[1]}_{\theta\varphi\varphi}}{\partial \varphi} \\ +\frac{1}{r}\left(4\tau^{[1]}_{r\theta\varphi} + 2\tau^{[1]}_{\theta\theta\varphi}\cot\theta - \tau^{[1]}_{\varphi\varphi\varphi}\cot\theta\right) \\ +\frac{1}{2}\left(\frac{1}{r}\frac{\partial m_{r\theta}}{\partial \theta} - \frac{\partial m_{\theta\theta}}{\partial r} + \frac{m_{rr} - m_{\theta\theta}}{r}\right) \end{array}\right)$$

$$\psi_{\varphi r} = \sigma_{\varphi r} - \left(\begin{array}{l} \frac{\partial p_\varphi}{\partial r} + \frac{\partial \tau^{[1]}_{rr\varphi}}{\partial r} + \frac{1}{r}\frac{\partial \tau^{[1]}_{r\theta\phi}}{\partial \theta} \\ +\frac{1}{r\sin\theta}\frac{\partial \tau^{[1]}_{rr\varphi}}{\partial \varphi} \\ +\frac{1}{r}\left(\begin{array}{l} 3\tau^{[1]}_{rr\varphi} - \tau^{[1]}_{\varphi\varphi\varphi} - \tau^{[1]}_{\theta\theta\varphi} \\ +2\tau^{[1]}_{r\theta\varphi}\cot\theta \end{array}\right) \\ +\frac{1}{2}\left(\begin{array}{l} \frac{1}{r\sin\theta}\frac{\partial m_{\theta\varphi}}{\partial \varphi} - \frac{1}{r}\frac{\partial m_{\varphi\varphi}}{\partial \theta} + \\ \frac{1}{r}(m_{r\theta} + m_{\theta\theta}\cot\theta \\ -m_{\varphi\varphi}\cot\theta) \end{array}\right) \end{array}\right)$$

$$\psi_{\varphi\theta} = \sigma_{\varphi\theta} - \left(\begin{array}{l} \frac{1}{r}\frac{\partial p_\varphi}{\partial \theta} + \frac{\partial \tau^{[1]}_{r\theta\varphi}}{\partial r} + \frac{1}{r}\frac{\partial \tau^{[1]}_{\theta\theta\phi}}{\partial \theta} \\ +\frac{1}{r\sin\theta}\frac{\partial \tau^{[1]}_{\theta\varphi\varphi}}{\partial \varphi} \\ +\frac{1}{r}\left(4\tau^{[1]}_{r\theta\varphi} + 2\tau^{[1]}_{\theta\theta\varphi}\cot\theta - \tau^{[1]}_{\varphi\varphi\varphi}\cot\theta\right) \\ +\frac{1}{2}\left(\begin{array}{l} \frac{\partial m_{\varphi\varphi}}{\partial r} - \frac{1}{r\sin\theta}\frac{\partial m_{r\varphi}}{\partial \varphi} \\ -\frac{1}{r}(m_{rr} + m_{r\theta}\cot\theta - m_{\varphi\varphi}) \end{array}\right) \end{array}\right)$$

10.57647/jsm.2026.1801.01

$$\psi_{\varphi\varphi} = \sigma_{\varphi\varphi} - \begin{pmatrix} \frac{1}{r\sin\theta}\frac{\partial p_\varphi}{\partial \varphi} + \frac{1}{r}(p_\varphi + p_\varphi \cot\theta) \\ + \frac{\partial \tau^{[1]}_{r\varphi\phi}}{\partial r} + \frac{1}{r}\frac{\partial \tau^{[1]}_{\theta\varphi\varphi}}{\partial \theta} + \frac{1}{r\sin\theta}\frac{\partial \tau^{[1]}_{\varphi\varphi\varphi}}{\partial \varphi} \\ + \frac{1}{r}\left(4\tau^{[1]}_{r\varphi\varphi} + 3\tau^{[1]}_{\theta\varphi\varphi}\cot\theta\right) \\ + \frac{1}{2}\left(\frac{1}{r}\frac{\partial m_{r\varphi}}{\partial \theta} - \frac{\partial m_{\theta\varphi}}{\partial r} - \frac{m_{\theta\varphi}}{r}\right) \end{pmatrix} \quad (6)$$

In the above relationships, the terms σ, p, τ and m are defined as follows:

$$\begin{aligned} \sigma_{ij} &= \lambda\varepsilon_{kk}\delta_{ij} + 2\mu\varepsilon_{ij} \\ p_i &= 2\mu l_0^2\gamma_1 \\ \tau^{[1]}_{ijk} &= 2\mu l_1^2\eta^{[1]}_{ijk} \\ m_{ij} &= 2\mu l_2^2\chi^{[s]}_{ij} \end{aligned} \quad (7)$$

The relationships of the Strain-Displacement for small shape changes in the theory of couple stress in spherical coordinates are expressed as follows [24]:

$$\begin{aligned} \varepsilon_{rr} &= \frac{\partial u_r}{\partial r} \\ \varepsilon_{\theta\theta} &= \frac{1}{r}\left(\frac{\partial u_\theta}{\partial \theta} + u_r\right) \\ \varepsilon_{\varphi\varphi} &= \frac{1}{r\sin\theta}\frac{\partial u_\varphi}{\partial \varphi} + \frac{u_r}{r} + \frac{u_\theta}{r}\cot\theta \\ \varepsilon_{r\theta} &= \frac{1}{2}\left(\frac{1}{r}\frac{\partial u_r}{\partial \theta} + \frac{\partial u_\theta}{\partial r} - \frac{u_\theta}{r}\right) \\ \varepsilon_{r\varphi} &= \frac{1}{2}\left(\frac{1}{r\sin\theta}\frac{\partial u_r}{\partial \varphi} + \frac{\partial u_\varphi}{\partial r} - \frac{u_\varphi}{r}\right) \end{aligned} \quad (8)$$

$$\varepsilon_{\theta\varphi} = \frac{1}{2}\left(\frac{1}{r\sin\theta}\frac{\partial u_\theta}{\partial \varphi} + \frac{1}{r}\frac{\partial u_\varphi}{\partial \theta} - \frac{u_\varphi}{r}\cot\theta\right) \quad (9)$$

In order to extract the coupled stress equations of FGM in spherical coordinates and in terms of displacement components, the coefficients of the mechanical properties of the FGM sphere are utilized in the form of a power function dependent on the radius r, based on the Tanigawa model [25, 26], as follows:

$$\begin{aligned} \lambda &= \lambda_\circ r^{m_1} \\ \mu &= \mu_\circ r^{m_2} \end{aligned} \quad (10)$$

In the above relations, $\mu_\circ$and $\lambda_\circ$ the constants are Lamé. By substituting the Eqs. (8)-(10) into Eq. (7) the radial, circumferential and shear stresses in terms of displacement components are obtained as,

$$\begin{aligned} \sigma_{rr} &= (3\lambda_\circ r^{m_1} + 2\mu_\circ r^{m_2})\left\{\frac{\partial u_r}{\partial r}\right\} \\ \sigma_{r\theta} &= 2\mu_\circ r^{m_2}\left\{\frac{1}{2}\left(\frac{1}{r}\frac{\partial u_r}{\partial \theta} + \frac{\partial u_\theta}{\partial r} - \frac{u_\theta}{r}\right)\right\} \\ \sigma_{r\varphi} &= 2\mu_\circ r^{m_2}\left\{\frac{1}{2}\left(\frac{1}{r\sin\theta}\frac{\partial u_r}{\partial \varphi} + \frac{\partial u_\varphi}{\partial r} - \frac{u_\varphi}{r}\right)\right\} \\ \sigma_{\theta\theta} &= (3\lambda_\circ r^{m_1} + 2\mu_\circ r^{m_2})\left\{\frac{1}{r}\left(\frac{\partial u_\theta}{\partial \theta} + u_r\right)\right\} \\ \varepsilon_{r\varphi} &= \frac{1}{2}\left(\frac{1}{r\sin\theta}\frac{\partial u_r}{\partial \varphi} + \frac{\partial u_\varphi}{\partial r} - \frac{u_\varphi}{r}\right) \\ \sigma_{\varphi r} &= 2\mu_\circ r^{m_2}\left\{\frac{1}{2}\left(\frac{1}{r\sin\theta}\frac{\partial u_r}{\partial \varphi} + \frac{\partial u_\varphi}{\partial r} - \frac{u_\varphi}{r}\right)\right\} \\ \sigma_{\varphi\theta} &= 2\mu_\circ r^{m_2}\left\{\frac{1}{2}\left(\frac{1}{r\sin\theta}\frac{\partial u_\theta}{\partial \varphi} + \frac{1}{r}\frac{\partial u_\varphi}{\partial \theta} - \frac{u_\varphi}{r}\cot\theta\right)\right\} \\ \sigma_{\varphi\varphi} &= 3\lambda_\circ r^{m_1}\left\{\frac{1}{r\sin\theta}\frac{\partial u_\varphi}{\partial \varphi} + \frac{u_r}{r} + \frac{u_\theta}{r}\cot\theta\right\} \\ &\quad + 2\mu_\circ r^{m_2}\left\{\frac{1}{r\sin\theta}\frac{\partial u_\varphi}{\partial \varphi} + \frac{u_r}{r} + \frac{u_\theta}{r}\cot\theta\right\} \end{aligned} \quad (11)$$

$$m_{r\varphi} = 2\mu_\circ r^{m_2} l_2^2 \left\{ \chi^{[s]}_{r\varphi}\frac{1}{4}\begin{pmatrix} -\frac{1}{r}\frac{\partial^2 u_r}{\partial r\partial \theta} + \frac{\partial^2 u_\theta}{\partial r^2} \\ -\frac{1}{r^2\sin^2\theta}\frac{\partial^2 u_\theta}{\partial \varphi^2} \\ +\frac{1}{r^2\sin\theta}\frac{\partial^2 u_\varphi}{\partial \varphi\partial \theta} \\ +\frac{2}{r^2}\frac{\partial u_r}{\partial \theta} + \frac{\cot\theta}{r^2\sin\theta}\frac{\partial u_\varphi}{\partial \varphi} \\ -\frac{2u_\theta}{r^2} \end{pmatrix} \right\} \quad (12)$$

$$m_{rr} = 2\mu_{\circ} r^{m_2} l_2^2 \left\{ \frac{1}{2} \left(\begin{array}{l} -\dfrac{1}{r\sin\theta}\dfrac{\partial^2 u_\theta}{\partial r \partial \varphi} + \dfrac{1}{r}\dfrac{\partial^2 u_\varphi}{\partial r \partial \theta} \\ + \dfrac{1}{r^2 \sin\theta}\dfrac{\partial u_\theta}{\partial \varphi} \\ + \dfrac{\cot\theta}{r}\dfrac{\partial u_\varphi}{\partial r} - \dfrac{1}{r^2}\dfrac{\partial u_\varphi}{\partial \theta} \\ - \dfrac{u_\varphi}{r^2}\cot\theta \end{array} \right) \right\}$$

$$m_{r\theta} = 2\mu_{\circ} r^{m_2} l_2^2 \left\{ \frac{1}{4} \left(\begin{array}{l} \dfrac{1}{r\sin\theta}\dfrac{\partial^2 u_r}{\partial r \partial \varphi} - \dfrac{1}{r^2\sin\theta}\dfrac{\partial^2 u_\theta}{\partial \theta \partial \varphi} \\ -\dfrac{\partial^2 u_\varphi}{\partial r^2} + \dfrac{1}{r^2}\dfrac{\partial^2 u_\varphi}{\partial \theta^2} - \dfrac{2}{r^2\sin\theta}\dfrac{\partial u_r}{\partial \varphi} \\ + \dfrac{\cot\theta}{r^2\sin\theta}\dfrac{\partial u_\theta}{\partial \varphi} + \dfrac{\cot\theta}{r^2}\dfrac{\partial u_\varphi}{\partial \theta} \\ + \dfrac{2u_\varphi}{r^2} - \dfrac{u_\varphi}{r^2\sin^2\theta} \end{array} \right) \right\}$$

$$m_{\theta\theta} = 2\mu_{\circ} r^{m_2} l_2^2 \left\{ \frac{1}{2} \left(\begin{array}{l} \dfrac{1}{r^2\sin\theta}\dfrac{\partial^2 u_r}{\partial \theta \partial \varphi} - \dfrac{1}{r}\dfrac{\partial^2 u_\varphi}{\partial r \partial \theta} \\ - \dfrac{\cot\theta}{r^2\sin\theta}\dfrac{\partial u_r}{\partial \varphi} \\ - \dfrac{1}{r^2\sin\theta}\dfrac{\partial u_\theta}{\partial \varphi} + \dfrac{u_\varphi}{r^2}\cot\theta \end{array} \right) \right\}$$

$$m_{\theta\varphi} = 2\mu_{\circ} r^{m_2} l_2^2 \left\{ \frac{1}{4} \left(\begin{array}{l} -\dfrac{1}{r}\dfrac{\partial^2 u_r}{\partial \theta^2} + \dfrac{1}{r^2\sin^2\theta}\dfrac{\partial^2 u_r}{\partial \varphi^2} \\ + \dfrac{1}{r}\dfrac{\partial^2 u_\theta}{\partial r \partial \theta} - \dfrac{1}{r\sin\theta}\dfrac{\partial^2 u_\varphi}{\partial r \partial \varphi} \\ + \dfrac{\cot\theta}{r^2}\dfrac{\partial u_r}{\partial \theta} - \dfrac{\cot\theta}{r}\dfrac{\partial u_\theta}{\partial r} \\ + \dfrac{1}{r^2}\dfrac{\partial u_\theta}{\partial \theta} - \dfrac{1}{r^2\sin\theta}\dfrac{\partial u_\varphi}{\partial \varphi} \\ - \dfrac{u_\theta}{r^2}\cot\theta \end{array} \right) \right\}$$

$$m_{\varphi\varphi} = 2\mu_{\circ} r^{m_2} l_2^2 \left\{ \frac{1}{2} \left(\begin{array}{l} -\dfrac{1}{r^2\sin\theta}\dfrac{\partial^2 u_r}{\partial \theta \partial \varphi} \\ + \dfrac{1}{r\sin\theta}\dfrac{\partial^2 u_\theta}{\partial r \partial \varphi} \\ + \dfrac{\cot\theta}{r^2\sin\theta}\dfrac{\partial u_r}{\partial \varphi} \\ - \dfrac{\cot\theta}{r}\dfrac{\partial u_\varphi}{\partial r} + \dfrac{1}{r^2}\dfrac{\partial u_\varphi}{\partial \theta} \end{array} \right) \right\} \tag{13}$$

Then, the couple stress Navier-Stokes equations for the FGM in three-dimensional spherical coordinates u_r, u_θ and u_φ and their derivatives in terms of r, $\theta$and φ are derived by substituting Eqs. (11)-(13) into Eqs. (4)-(6). Due to the complexity of the resulting expressions in the Navier-Stokes equations, the following expression $\psi_{ij}(i,j = r,\theta,\varphi)$ is defined as:

$$\psi_{ij} = \zeta_{ij}(u_r, u_\theta, u_\varphi, \frac{\partial}{\partial r}, \frac{\partial}{\partial \theta}, \frac{\partial}{\partial \varphi}) \tag{14}$$

Thus, the stress Navier-Stokes equations for the FGM in three-dimensional spherical coordinates are given as follows,

$$\begin{array}{l} \dfrac{\partial}{\partial r}(\zeta_{rr}) + \dfrac{1}{r}\dfrac{\partial}{\partial \theta}(\zeta_{\theta r}) + \dfrac{1}{r\sin\theta}\dfrac{\partial}{\partial \varphi}(\zeta_{\varphi r}) \\ + \dfrac{1}{r}\left(2\zeta_{rr} - \zeta_{\theta\theta} - \zeta_{\varphi\varphi} + \zeta_{\theta r}\cot\theta\right) + f_r = 0 \end{array} \tag{15}$$

$$\begin{array}{l} \dfrac{\partial}{\partial r}(\zeta_{r\theta}) + \dfrac{1}{r}\dfrac{\partial \psi_{\theta\theta}}{\partial \theta}(\zeta_{\theta\theta}) + \dfrac{1}{r\sin\theta}\dfrac{\partial}{\partial \varphi}(\zeta_{\varphi\theta}) + \\ \dfrac{1}{r}\left(2\zeta_{r\theta} + \zeta_{\theta r} + (\zeta_{\theta\theta} - \zeta_{\varphi\varphi})\cot\theta\right) + f_\theta = 0 \end{array} \tag{16}$$

$$\begin{array}{l} \dfrac{\partial}{\partial r}(\zeta_{r\varphi}) + \dfrac{1}{r}\dfrac{\partial}{\partial \theta}(\zeta_{\theta\varphi}) + \dfrac{1}{r\sin\theta}\dfrac{\partial}{\partial \varphi}(\zeta_{\varphi\varphi}) \\ + \dfrac{1}{r}\left(2\zeta_{r\varphi} + \zeta_{\varphi r} + \zeta_{\varphi\theta}\cot\theta\right) + f_\varphi = 0 \end{array} \tag{17}$$

8. Research methodology and introduction of the generalized differential quadrature method (GDQ)

The GDQ method is a numerical technique developed to estimate spatial derivatives in various engineering problems. This method operates based on a weighted approach and has the capability to be generalized to achieve more accurate results in dynamic and static problems. GDQ offers higher accuracy and reduced computational time compared to traditional methods such as finite difference and finite element methods [27]. In this approach, the function is considered within the domain under investigation, and the derivative of the function at a point will be as follows:

8.1. Domain of discretization

The Generalized Differential Quadrature (GDQ) method based on the least-squares formulation has been used for the discretization of the governing Eqs. (18)-(20). In most of the conducted research, two distributions, uniform and non-uniform (Chebyshev-Gauss-Lobatto), are utilized as follows:

$$x_i|x_i =$$

$$x_1+\frac{1}{2}(1-x_1)\left(\frac{i-1}{N-1}\right) \qquad 1 \le i \le N$$

$$x_i|x_i = x_1+\frac{1}{2}(1-x_1) \tag{18}$$

$$\left[1-cos\left(\frac{i-1}{N-1}\right)\pi\right] \qquad 1 \le i \le N$$

In this article, a uniform grid distribution is selected to enhance the convergence rate and numerical accuracy of the solution. By employing the differential quadrature method, there are no limitations in applying boundary conditions, and various boundary conditions can be implemented at any edge of the sector. Due to the complexity of the three-dimensional coupled stress equations in a three-dimensional FGM sphere, we consider the numerical results of the problem in two dimensions domain. Therefore, the grid points are uniformly distributed in spherical coordinates.

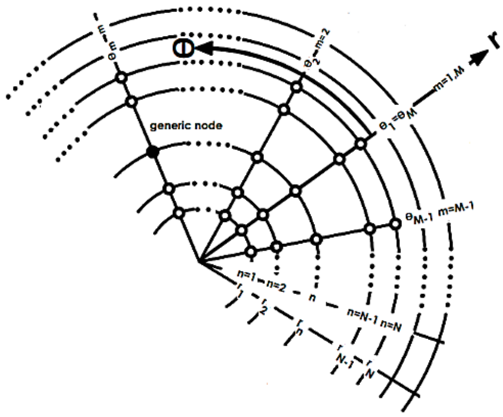

Figure 1. Discrete polar domain

Figure 1 illustrates the discretized domain, where the grid points are represented by radial rays and concentric circles. The total number of the grid point m of the discrete domain is obtained from the Eq. (18).

8.2. Numerical derivatives

The weighting coefficients are classically defined $L_n(x)$ as the values of the n-th derivative of the Lagrange interpolation polynomials $x = x_n$.

$$g = g(m,n) = (m-1)N+n$$
$$1 \le m \le M, 1 \le n \le N \tag{19}$$

As shown by expressions Eq. (19), the discrete set of function values $\{y(x)|1 \le i \le N\}$ can approximate the function values at x through using a series of Lagrange interpolation polynomials.$\{L_n(x)|1 \le i \le N\}$.

Moreover, the first derivative of the functioncan can also be approximated using the set of GDQ coefficients, which are defined as follows:

$$y(x) = \sum_{n=1}^{N} y_n L_n(x)$$

$$L_n(x) \equiv \frac{\prod_{\substack{m=1\\m\neq n}}^{N}(x-x_m)}{(x-x_n)\prod_{\substack{m=1\\m\neq n}}^{N}(x_n-x_m)} \tag{20}$$

$$y'(x) = \sum_{n=}^{N} y_n\, L'_n(x)$$

$$L'_n(x) \equiv \frac{1}{\prod_{\substack{m=1\\m\neq n}}^{N}(x_n-x_m)}\sum_{k=1}^{N}\prod_{\substack{m=1\\m\neq n\\m\neq k}}^{N}(x-x_m)$$

The vectors related to the numerical derivative coefficients A_i, B_i, C_i and D_i are presented as follows for order 0 to 4:

$$A_i = \left[a_i^1 \quad a_i^1 \quad \dots \quad a_i^k \qquad a_i^{N-1} \quad a_i^N\right]^T$$
$$B_i = \left[b_i^1 \quad b_i^1 \quad \dots \quad b_i^k \qquad b_i^{N-1} \quad b_i^N\right]^T$$
$$C_i = \left[c_i^1 \quad c_i^1 \quad \dots \quad c_i^k \qquad c_i^{N-1} \quad c_i^N\right]^T \tag{21}$$
$$D_i = \left[d_i^1 \quad d_i^1 \quad \dots \quad d_i^k \qquad d_i^{N-1} \quad d_i^N\right]^T$$

In Eq. (21), the coefficients related to the first through fourth derivatives, namely a_i^k,b_i^k, c_i^k and d_i^k, are defined based on the GDQ method (22) as follows:

$$a_i^k \equiv$$
$$\frac{\prod_{\substack{m=1\\m\neq i}}^{N}(x_i-x_m)}{(x_i-x_k)\prod_{\substack{m=1\\m\neq k}}^{N}(x_k-x_m)}, a_i^k \equiv -\sum_{\substack{m=1\\m\neq i}}^{N} a_i^m$$

$$b_i^k \equiv$$
$$\frac{\prod_{\substack{m=1\\m\neq i}}^{N}(x_i-x_m)}{(x_i-x_k)\prod_{\substack{m=1\\m\neq k}}^{N}(x_k-x_m)}, b_i^k \equiv -\sum_{\substack{m=1\\m\neq i}}^{N} b_i^m$$

$$c_i^k \equiv \tag{22}$$
$$\frac{\prod_{\substack{m=1\\m\neq i}}^{N}(x_i-x_m)}{(x_i-x_k)\prod_{\substack{m=1\\m\neq k}}^{N}(x_k-x_m)}, c_i^k \equiv -\sum_{\substack{m=1\\m\neq i}}^{N} c_i^m$$

$$d_i^k \equiv$$
$$\frac{\prod_{\substack{m=1\\m\neq i}}^{N}(x_i-x_m)}{(x_i-x_k)\prod_{\substack{m=1\\m\neq k}}^{N}(x_k-x_m)}, d_i^k \equiv -\sum_{\substack{m=1\\m\neq i}}^{N} d_i^m$$

According to Eq. (14), the field variables are denoted by u_r, u_θ and u_φ. If we represent a generic field variable as$\sigma$and let $\sum$denote the total number of field variables $(1 \leq \sigma \leq \sum)$, Then we have [28]:

$$LS\sigma_m^n = H_1^{n,N} LS\sigma_m = H_1^{m,M} LS\sigma^n \tag{23}$$

In the above relation $S\sigma_m^n$, the field variableσ is located at the n-th circular node and the m-th radial ray.
To extract the σ -th row $N \times 1$from the combination $(\Sigma N \times 1)$, Eq. (23) is used [28].
The expression $H_N^{\sigma,\Sigma}$is defined as follows:

$$H_N^{\sigma,\Sigma} = [0_{N\times(\sigma-1)N} \quad I_{N\times N} \quad 0_{N\times(\Sigma-\sigma)N}] \tag{24}$$

For the given values$N = 1, \sigma = n$ and $\Sigma = N$ the Eq. (24) is reduced to a simplified form $H_1^{m,M}$.
Furthermore, $Ls\sigma^n$the field variableσ -th along the entire circle n-th, $Ls\sigma_m$the field variableσ -th along the entire ray m -th and$LS\sigma$ the field variable σ- th along all nodes are defined as follows [28]:

$$\begin{aligned} Ls\sigma_m &= H_N^{m,M} Ls\sigma \\ Ls\sigma^n &= R^n Ls\sigma \\ Ls\sigma &= H_{MN}^{\sigma,\Sigma} Ls \end{aligned} \tag{25}$$

In the above relationships, the symbols LS, $Ls\sigma$ and $R^n$are represented as follows [28]:

$$LS = \begin{bmatrix} LS1 \\ \vdots \\ LS\sigma \\ \vdots \\ LS\Sigma \end{bmatrix}_{\Sigma MN\times 1}$$

$$Ls\sigma = \begin{bmatrix} LS\sigma_1 \\ \vdots \\ LS\sigma_m \\ \vdots \\ LS\sigma_M \end{bmatrix}_{MN\times 1} \tag{26}$$

$$R^n = \begin{bmatrix} H_1^{g(1,n),MN} \\ \vdots \\ H_1^{g(m,n),MN} \\ \vdots \\ H_1^{g(M,n),MN} \end{bmatrix}_{M\times MN}$$

By substituting relations (25) into Eq. (23), we obtain [28]:

$$\begin{aligned} S\sigma_m^n &= H_1^{n,N} H_N^{m,M} H_{MN}^{\sigma,\Sigma} Ls \\ &= H_1^{m,M} R^n H_{MN}^{\sigma,\Sigma} Ls \end{aligned} \tag{27}$$

The partial derivatives $LS\sigma_m^n$with respect to $r$and θcan be expressed as follows [28]:

$$\begin{aligned} &\left[\frac{\partial(LS\sigma_m^n)}{\partial r} \quad \frac{\partial^2(LS\sigma_m^n)}{\partial r^2} \quad \frac{\partial^3(LS\sigma_m^n)}{\partial r^3} \quad \frac{\partial^4(LS\sigma_m^n)}{\partial r^4}\right] = [A^n \quad B^n \quad C^n \quad D^n] H_N^{m,M} H_{MN}^{\sigma,\Sigma} LS \\ &\left[\frac{\partial(LS\sigma_m^n)}{\partial \theta} \quad \frac{\partial^2(LS\sigma_m^n)}{\partial \theta^2} \quad \frac{\partial^3(LS\sigma_m^n)}{\partial \theta^3} \quad \frac{\partial^4(LS\sigma_m^n)}{\partial \theta^4}\right] = [A^m \quad B^m \quad C^m \quad D^m] R^n H_{MN}^{\sigma,\Sigma} LS \\ &\left[\frac{\partial^2(LS\sigma_m^n)}{\partial r\partial\theta} \quad \frac{\partial^3(LS\sigma_m^n)}{\partial r^2\partial\theta} \quad \frac{\partial^3(LS\sigma_m^n)}{\partial r\partial\theta^2} \quad \frac{\partial^4(LS\sigma_m^n)}{\partial r^2\partial\theta^2} \quad \frac{\partial^4(LS\sigma_m^n)}{\partial r^3\partial\theta} \quad \frac{\partial^4(Ls\sigma_m^n)}{\partial r\partial\theta^3}\right] = \\ &[A^n Ar^m \quad B^n Ar^m \quad A^n Br^m \quad B^n Br^m \quad C^n Ar^m \quad A^n Cr^m] H_{MN}^{\sigma,\Sigma} LS \end{aligned} \tag{28}$$

The coefficients A^n, B^n, C^n, D^n, Ar^m, Br^m and Cr^m appearing in Eq. (28) are defined as follows:

$$\begin{aligned} &A^n = [A_1^n \quad A_2^n \quad \dots \quad A_N^n]_{1\times N} \qquad B^n = [B_1^n \quad B_2^n \quad \dots \quad B_N^n]_{1\times N} \\ &C^n = [C_1^n \quad C_2^n \quad \dots \quad C_N^n]_{1\times N} \qquad D^n = [D_1^n \quad D_2^n \quad \dots \quad D_N^n]_{1\times N} \\ &Ar^m = \begin{bmatrix} A^m R^1 \\ \vdots \\ A^m R^1 \\ \vdots \\ A^m R^N \end{bmatrix}_{N\times MN} \qquad Br^m = \begin{bmatrix} B^m R^1 \\ \vdots \\ B^m R^1 \\ \vdots \\ B^m R^N \end{bmatrix}_{N\times MN} \qquad Cr^m = \begin{bmatrix} C^m R^1 \\ \vdots \\ C^m R^1 \\ \vdots \\ C^m R^N \end{bmatrix}_{N\times MN} \end{aligned} \tag{29}$$

8.3. Discrete boundary conditions

The boundary conditions for a two-dimensional FGM microsphere subjected to internal pressure are defined as follows [29]:

$$\begin{cases} \sigma_{rr} - l^2\left[\dfrac{d^2\sigma_{rr}}{dr^2} + \dfrac{1}{r}\left(\dfrac{d\sigma_{rr}}{dr} - \dfrac{d\sigma_{\theta\theta}}{dr}\right) - \dfrac{2}{r^2}(\sigma_{rr} - \sigma_{\theta\theta})\right]_{r=r_i} = -P_i \\ l^2 \dfrac{d\sigma_{rr}}{dr}\Big|_{r=r_i} = 0 \\ \sigma_{rr} - l^2\left[\dfrac{d^2\sigma_{rr}}{dr^2} + \dfrac{1}{r}\left(\dfrac{d\sigma_{rr}}{dr} - \dfrac{d\sigma_{\theta\theta}}{dr}\right) - \dfrac{2}{r^2}(\sigma_{rr} - \sigma_{\theta\theta})\right]_{r=r_o} = -P_o \\ l^2 \dfrac{d\sigma_{rr}}{dr}\Big|_{r=r_o} = 0 \end{cases} \tag{30}$$

For discretize, The Navier equations Eqs. (15)-(17) and the boundary conditions Eq. (30) are substituted into the relations (28). Using the GDQ method to static problems results in a system of algebraic equations, where the unknowns correspond to the values of the function at the nodal points.

9. Numerical results and discussion

In order to evaluate the accuracy and physical consistency of the proposed analytical-numerical model, the governing equations based on the modified couple stress theory (MCST) are solved using the generalized differential quadrature (GDQ) method for the functionally graded hollow sphere. The material properties are assumed to vary in the radial direction according to a power-law distribution characterized by the material profile index m. The results are compared with the classical theory of elasticity and the available analytical data reported by Poultangari et al. [30] for validation. Numerical analysis was performed for a sphere with an inner radius r_i=0.4m and an outer radius r_o= 0.5m. The loading was considered as a non-uniform internal pressure P_i=400cos(4ϴ) and zero external pressure. The material properties were defined based on a power law with the form m=1,2 and the scale length parameter in couple stress theory l = 0.1 µm, representing a macroscale geometry (l/ro ≈ 2×10−7). The Poisson's ratio is assumed to be constant at 0.3, while E(a) is defined as 200 GPa, respectively. For simplicity, the material properties are considered equal (so that m3 = m1 = m2 = m). The mechanical boundary conditions are shown in Table 1.

Table 1. Boundary conditions for Elastic Hollow sphere FGM [30]

r_i	r_o	P_i	P_o	ν	N_r	N_Θ
0.4m	0.5m	400cos 4ϴ	0	0.3	24	24

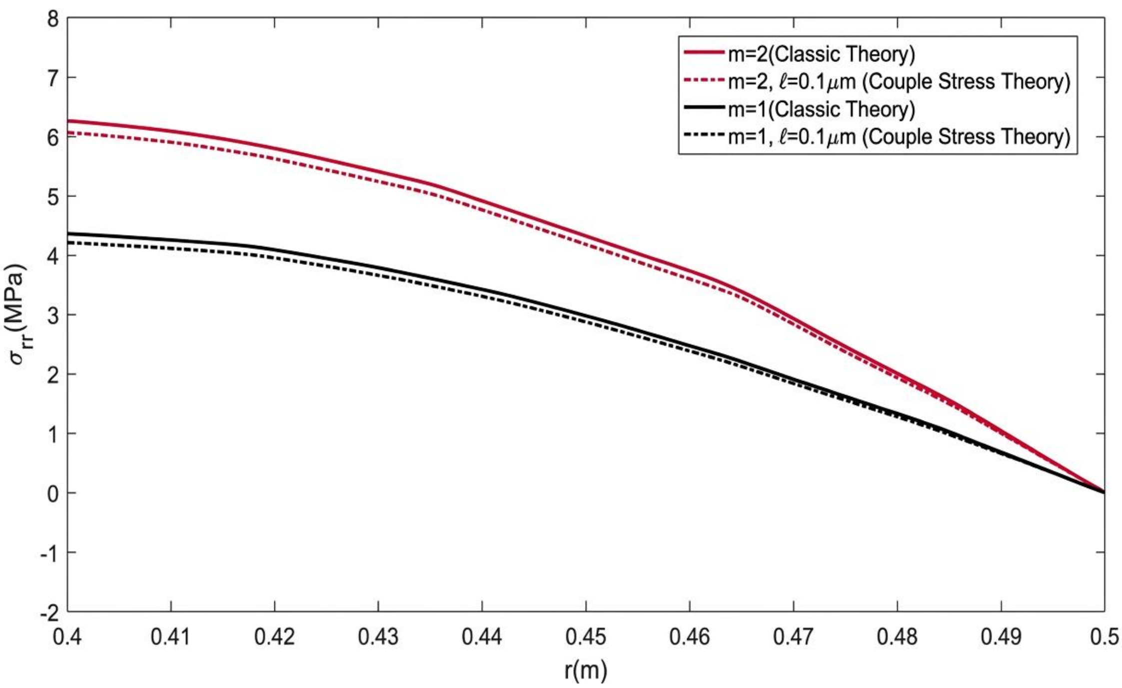

Figure 2. Radial stress: comparison between classical and couple stress theories

10.57647/jsm.2026.1801.01

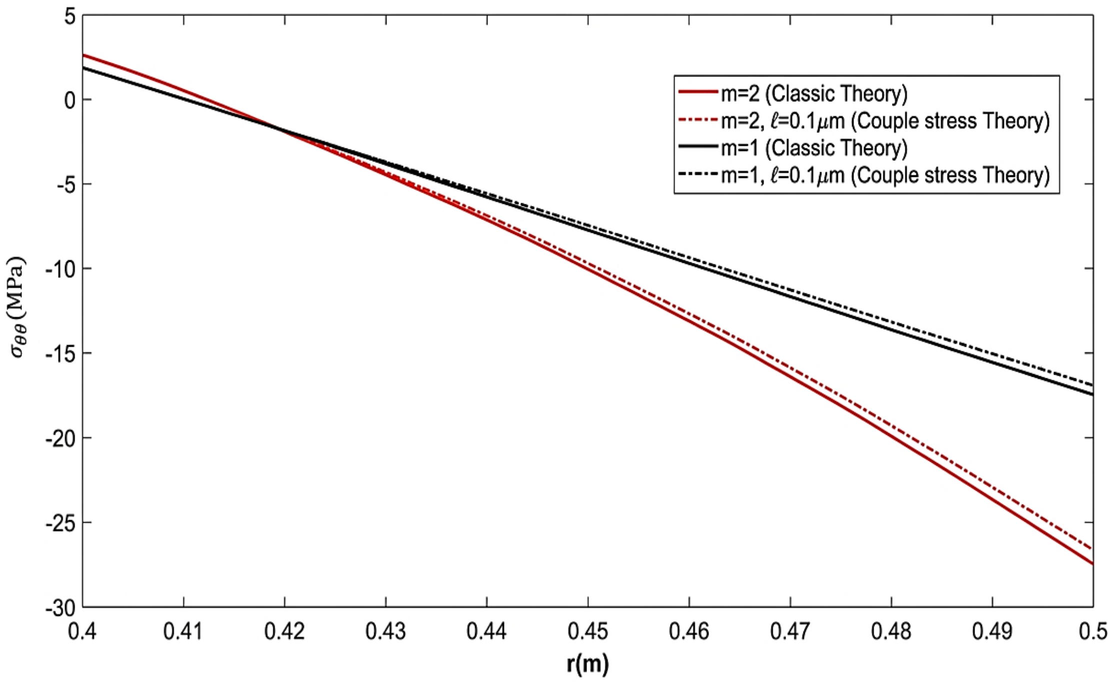

Figure 3. Circumferential stress: comparison between classical and couple stress theories

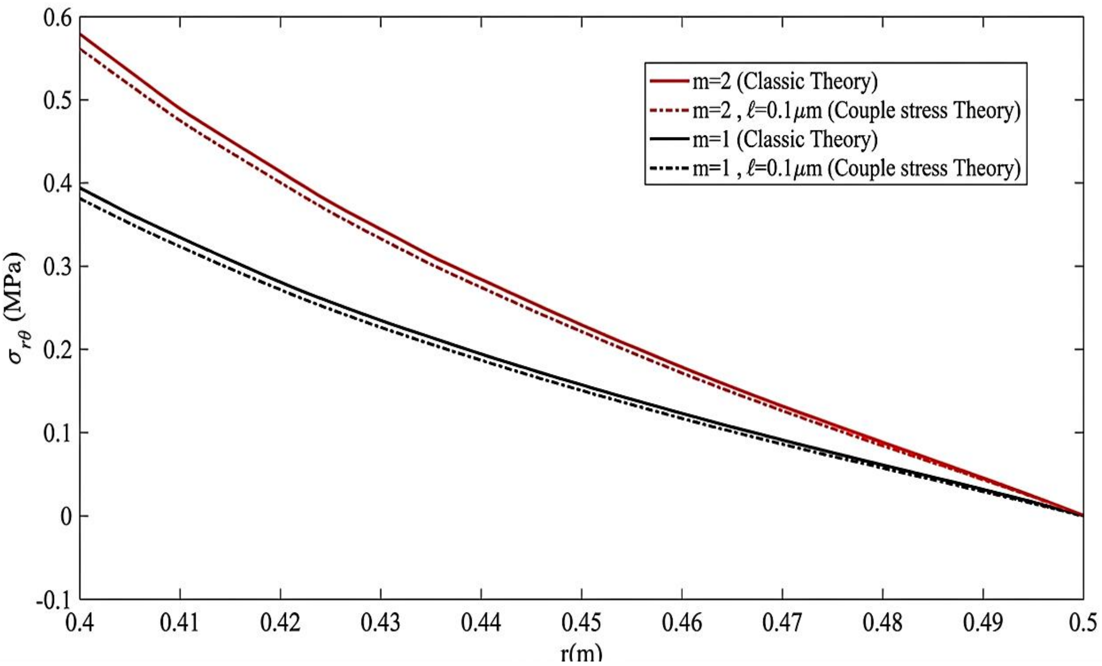

Figure 4. Shear stress: comparison between classical and couple stress theories

The governing equations were discretized and solved using the generalized differential quadrature (GDQ) method, which provides high accuracy in calculating derivatives and applying boundary conditions. The three main components of the response were investigated, including radial stress σ_{rr}, circumferential stress $\sigma_{\theta\theta}$, and shear stress $\sigma_{r\theta}$.

Numerical convergence was achieved with 24 grid points, confirming the accuracy and stability of the GDQ scheme. For all cases, the difference between MCST and classical predictions remained below 1%, which is consistent with the physical expectation that size effects vanish at macroscopic scales.

Figure 2 At the inner surface (r=0.4 m) the max of σ_{rr} is about 4.5 MPa for m=1 and 6.2 MPa for m=2 in the classical theory (l=0). For MCST (l=0.1 μm), there is a slight reduction in these values to around 4.2 MPa (for m =1) and 6.0 MPa (for m =2). However, in the σ_{rr} components, the values decrease monotonically to zero at the outer boundary (r =0.5m), as expected. Increasing m shows a marked increase in σ_{rr}, while a small nonzero value of l shows a small reduction in σ_{rr}. This trend agrees

10.57647/jsm.2026.1801.01

with Poultangari et al. [30], who reported that smaller gradation index yields lower stress magnitudes.

Figure 3 Near the inner radius, $\sigma_{\theta\theta}$ is tensile for m=2, approximately +3.2 MPa at r=0.4 m (classical theory), as opposed to around +2.7 MPa for m=1. With l=0.1 μm these tensile values slightly increase (to approximately +3.4 MPa and +3.0 MPa).

Toward the outer surface the hoop stress becomes compressive at r=0.5 m, $\sigma_{\theta\theta}$ is about−27 MPa for m=2 (classical) and −17.5 MPa for m=1 (classical). The MCST case (l>0) causes a slight reduction in the compressive value. Therefore, $\sigma_{\theta\theta}$ varies smoothly from a positive value at the inner surface to a negative value at the outer surface.

As in previous analyses, increasing values of m result in larger stress values, and a small value of l=0.1μm applies insignificant corrections. This trend agrees with the results obtained by Poultangari et al. in relation to tangential stress.

Figure 4 Shear stresses attained a higher value at the inner surface under the application of loads. For m=2 (classical) max of $\sigma_{r\theta}\approx$ 0.57 MPa at r=0.4 m, whereas for m=1 it is about 0.40 MPa. Introducing l=0.1 μm reduces these peaks slightly (≈0.56 MPa and 0.38 MPa). In all cases $\sigma_{r\theta}$ decays to zero at r=0.5 m. Whereas values of shear stresses are much lower than those of the stresses in both directions, signifying the moderate loading condition of a non-axisymmetric type.

Trends in variations of $\sigma_{r\theta}$ values match those of variations of stresses in directions r & θ; higher m causes a higher value of shear stress, where a small positive value of l gives a small decrement.

Material index and length scale effects: This is sensitive to the power-law index m as well as length scale parameter l.

A large m means that the values of stresses will increase (for example, peak σ_{rr} and $\sigma_{r\theta}$ rise by roughly 30–40% when m goes from 1 to 2). However, a small microstructural length scale of l = 0.1 μm leads to negligible effects of a few percent only, in which σrr and $\sigma_{r\theta}$ will decrease (due to increased hardness), as well as increasing $\sigma_{\theta\theta}$ slightly at the outer boundary. This agrees well with the findings of Poultangari et al. [30], who observed that a small value of power-law index leads to a reduction in radial, tangential, as well as shear stresses. A small microstructural length scale of MCST effectively makes the material harder.

Therefore, as expected, when $l \rightarrow 0$, the solution of MCST will be the same as that of classical elasticity theory.

In sum, the stress distribution curves (Figures 2–4) exhibit smooth, physically consistent behavior, and both qualitative trends and quantitative values match established analytical solutions.

10. Conclusion

In this study, the mechanical behavior of a functionally graded hollow sphere under non-uniform mechanical loading was analyzed using the scale-dependent couple stress theory and the generalized differential quadrature (GDQ) method. The results obtained highlight several key and innovative points:

10.1. Length scale and material gradation effects

It is observed that as the value of the material gradation index m is increased, the values of the radial stress, circumferential stress, as well as shear stresses, are substantially increased, while including the microstructure size parameter as l = 0.1 μm gives a small stiffening effect (slightly reducing stresses). As expected, in a convergence analysis done upon a 24-point grid, the solution is obtained with no appreciable error in solution. Also, under the limiting condition of sufficiently small values of l (in the macroscopic regime), as already illustrated earlier, the MCST solution, as expected, approaches that of the classical (elasticity theory).

10.2. Consistency of the model with real physics

A high accuracy of the results obtained from the proposed GDQ/MCST model has been found in comparison with the outcomes of the classical theory of elasticity. Also, in order to obtain the results, a discretization of 24 points has been used, as a result of which a convergence error of less than 2% has been observed. Moreover, a comparison of the obtained results with recent studies in this field, as presented by Poultangari et al. [30], has revealed that the mean error is less than 3%.

In addition, since the length scale parameter of the given material (l = 0.1 μm) is much smaller than the sphere’s characteristic dimensions (in the order of centimeters), the effects of couple stresses become physically insignificant. As a result, the solutions of the modified couple stress theory will be in agreement with those of the classical theory of elasticity, indicating full physical consistency between the above-mentioned theories.

10.3. Innovation and practical significance

The novelty of the research this research consists in the combination of couple stress theory with the GDQ numerical method applied to the analysis of functionally graded spheres under non-axial loading. This approach allows for the accurate investigation of scale effects, material gradients, and complex boundary conditions simultaneously while most of the previous studies haveonly examined symmetric or classical cases.

The results of this research can be used in the design of microscopic shells, MEMS components, and nanoscale FGM tanks where stress and stiffness distributions play a key role. Overall, the presented model, by simultaneously considering the effects of length scale and non-axial loading, has been able to provide a realistic and accurate behavior of the functionally graded sphere. This research can be the basis for the development of more advanced analytical and numerical models for the analysis of microscopic structures and smart materials in the future.

Authors Contribution
F.S. developed the theoretical formulation and performed the numerical simulations. M.J. supervised the research, contributed to the formulation and interpretation of the results, and revised the manuscript. M.Y.T. contributed to the problem definition, discussion of the numerical results, and editing of the manuscript. All authors read and approved the final manuscript.

Availability of data and materials
The datasets generated and/or analyzed during the current study are available from the corresponding author on reasonable request.

Conflict of interests
The authors declare no conflicts of interest.

References

[1] Mohammadi M, Rajabi M, Ghadiri M. Functionally graded materials (FGMs): A review of classifications, fabrication methods and their applications. Processing and Application of Ceramics. 2021. DOI: https://doi.org/10.2298/pac2104319m

[2] Alinaghizadeh F, Kadkhodayan M. Investigation of Nonlinear Bending Analysis of Moderately Thick Functionally Graded Material Sector Plates Subjected to Thermomechanical Loads by the GDQ Method. Journal of Engineering Mechanics-asce. 140:04014012 (2014). DOI: https://doi.org/10.1061/(ASCE)EM.1943-7889.0000715

[3] Pasha A, Rajaprakash BM. Fabrication and mechanical properties of functionally graded materials: A review. Materials Today: Proceedings. 2021. DOI:https://doi.org/10.1016/j.matpr.2021.09.066

[4] Du H, Lim MK, Lin R. Application of generalized differential quadrature method to structural problems. International Journal for Numerical Methods in Engineering. 37:1881–96 (1994). DOI: https://doi.org/10.1002/NME.1620371107

[5] Suresh S, Mortensen A, editors. Fundamentals of functionally graded materials: processing and thermomechanical behaviour of graded metals and metal-ceramic composites(1998). https://www.researchgate.net/publication/257555723_Fundamentals_of_Functionally_Graded_Materials

[6] Noori H, Jomehzadeh E. Length scale effect on vibration analysis of functionally graded kirchhoff and mindlin micro-plates. International Journal of Engineering, Transactions C: Aspects. 27(3):431–40 (2014). DOI: https://doi.org/10.5829/idosi.ije.2014.27.03c.11

[7] Yas MH, Shakeri M, Heshmati M, Mohammadi S. Layer-wise finite element analysis of functionally graded cylindrical shell under dynamic load. Journal of Mechanical Science and Technology. 25:597–604 (2011). DOI: https://doi.org/10.1007/s12206-011-0116-6

[8] Khaniki HB, Hashemi SH. Free vibration analysis of nonuniform microbeams based on modified couple stress theory: an analytical solution. International Journal of Engineering-Transactions B: Applications. 30(2):311–20 (2017). DOI: https://doi.org/10.5829/idosi.ije.2017.30.02b.19

[9] Tornabene F, Viola E. 2-D solution for free vibrations of parabolic shells using generalized differential quadrature method. European Journal of Mechanics A-solids. 27:1001–25 (2008). DOI:https://doi.org/10.1016/j.euromechsol.2007.12.007

[10] Wu C-P, Chang T-Y. A Review of Modified/Consistent Couple Stress and Strain Gradient Theories for Analyzing Static and Dynamic Behaviors of Functionally Graded Microscale Plates and Shells. Materials. 18 (2025). DOI: https://doi.org/10.3390/ma18194475

[11] Ravandi SAH, tadi z, Beni YT. Investigation of the Size Effect on the Nano-beam Type Piezoelectric Low Power Energy Harvesting. International Journal of Engineering. (2018). DOI: https://doi.org/10.5829/ije.2018.31.09c.15

[12] Forghani M, Abdellahi R, Esmaeili M, Alizadehsani R, Pławiak P. Modified Couple Stress Theory for nonlinear primary resonance of FG-GPLRC cylindrical shells in thermal environment. PLOS One. 20 (2025). DOI: https://doi.org/10.1371/journal.pone.0323442

[13] Rashvand K, Rezazadeh G, Madinei H. Effect of length-scale parameter on pull-in voltage and natural frequency of a micro-plate. International Journal of Engineering. 27(3):375–84 (2014). DOI:https://doi.org/10.5829/IDOSI.IJE.2014.27.03C.04

[14] Abazari AM, Safavi SM, Rezazadeh G, Fathalilou M. Couple stress effect on micro/nanocantilever-based capacitive gas sensor. Int J Eng. 29(6):852–61 (2016).

DOI: https://doi.org/10.5829/idosi.ije.2016.29.06c.15

[15] Farokhi H, Ghayesh MH. Modified couple stress theory in orthogonal curvilinear coordinates. Acta Mechanica. 230(3):851–69 (2019).
DOI: https://doi.org/10.1007/S00707-018-2331-Z

[16] Bleustein JL. Effects of micro-structure on the stress concentration at a spherical cavity. International Journal of Solids and Structures. 2(1):83–104 (1966).
DOI: https://doi.org/10.1016/0020-7683(66)90008-4

[17] Zhao J, Pedroso D. Strain gradient theory in orthogonal curvilinear coordinates. International Journal of Solids and Structures. 45(11-12):3507–20 (2008).
DOI:https://doi.org/10.1016/J.IJSOLSTR.2008.02.011

[18] Jomehzadeh E, Noori HR, Saidi AR. The size-dependent vibration analysis of micro-plates based on a modified couple stress theory. Physica E-low-dimensional Systems & Nanostructures. 43:877–83 (2011).
DOI: https://doi.org/10.1016/J.PHYSE.2010.11.005

[19] Nateghi A, Salamat-talab M, Rezapour J, Daneshian B. Size dependent buckling analysis of functionally graded micro beams based on modified couple stress theory. Applied Mathematical Modelling. 36:4971–87 (2012).
DOI:https://doi.org/10.1016/J.APM.2011.12.035

[20] Reddy J. microstructure-dependent couple stress theories of functionally graded beams. Journal of The Mechanics and Physics of Solids. 59:2382–99 (2011).
DOI: https://doi.org/10.1016/J.JMPS.2011.06.008

[21] Reddy J, Kim J. A nonlinear modified couple stress-based third-order theory of functionally graded plates. Composite Structures. 94:1128–43 (2012).
DOI:https://doi.org/10.1016/J.COMPSTRUCT.2011.10.006

[22] Sadeghi H, Baghani M, Naghdabadi R. Strain gradient elasticity solution for functionally graded micro-cylinders. International Journal of Engineering Science. 50(1):22–30 (2012).
DOI:https://doi.org/10.1016/J.IJENGSCI.2011.09.006

[23] Salamat-talab M, Shahabi F, Assadi A. Size dependent analysis of functionally graded microbeams using strain gradient elasticity incorporated with surface energy. Applied Mathematical Modelling. 37(1-2):507–26 (2013).
DOI: https://doi.org/10.1016/J.APM.2012.02.053

[24] Ashoori A, Mahmoodi MJ. The modified version of strain gradient and couple stress theories in general curvilinear coordinates. European Journal of Mechanics A-solids. 49:441–54 (2015).
DOI:https://doi.org/10.1016/J.EUROMECHSOL.2014.09.002

[25] Peng XL, Li XF. Thermoelastic analysis of a cylindrical vessel of functionally graded materials. International Journal of Pressure Vessels and Piping. 87:203–10 (2010).
DOI: https://doi.org/10.1016/J.IJPVP.2010.03.024

[26] Wang Z, Zhang Q, Xia L, Wu JT, Liu P. Stress Analysis and Parameter Optimization of an FGM Pressure Vessel Subjected to Thermo-Mechanical Loadings. Procedia Engineering. 130:374–89 (2015).
DOI:https://doi.org/10.1016/J.PROENG.2015.12.230

[27] Shu C, editor Differential Quadrature and Its Application in Engineering 2000.
DOI: https://doi.org/10.1007/978-1-4471-0407-0

[28] Rezaei M, Khorshidvand AR, Khorsandijou SM, Jabbari M. Influence of length scale parameter on nonlinear bending of functionally graded saturated porous rectangular microplates. Special Topics & Reviews in Porous Media: An International Journal. 13(2) (2022).
DOI:https://doi.org/10.1615/SpecialTopicsRevPorousMedia.2022040711

[29] Chu L, Dui G. Exact solutions for functionally graded micro-cylinders in first gradient elasticity. International Journal of Mechanical Sciences. 2018.
DOI:https://doi.org/10.1016/J.IJMECSCI.2018.09.011

[30] Poultangari R, Jabbari M, Eslami MR. Functionally graded hollow spheres under non-axisymmetric thermo-mechanical loads. International Journal of Pressure Vessels and Piping. 85:295–305 (2008).
DOI: https://doi.org/10.1016/J.IJPVP.2008.01.002